

This article was downloaded by:

On: 28 January 2011

Access details: *Access Details: Free Access*

Publisher *Taylor & Francis*

Informa Ltd Registered in England and Wales Registered Number: 1072954 Registered office: Mortimer House, 37-41 Mortimer Street, London W1T 3JH, UK



## Physics and Chemistry of Liquids

Publication details, including instructions for authors and subscription information:

<http://www.informaworld.com/smpp/title~content=t713646857>

### Electronic transport properties of liquid gallium-germanium alloys

M. Mayoufi<sup>a</sup>; F. Sar<sup>b</sup>; L. Anno<sup>b</sup>; J. G. Gasser<sup>b</sup>

<sup>a</sup> Laboratoire de Chimie des Matériaux Inorganiques, Université Badji-Mokhtar Annaba, 23000

Annaba, Algérie <sup>b</sup> Laboratoire de Physique des Milieux Denses (L.P.M.D), Université Paul Verlaine-Metz, cedex 3, France

**To cite this Article** Mayoufi, M. , Sar, F. , Anno, L. and Gasser, J. G.(2008) 'Electronic transport properties of liquid gallium-germanium alloys', *Physics and Chemistry of Liquids*, 46: 2, 191 – 201

**To link to this Article:** DOI: 10.1080/00319100701548327

**URL:** <http://dx.doi.org/10.1080/00319100701548327>

PLEASE SCROLL DOWN FOR ARTICLE

Full terms and conditions of use: <http://www.informaworld.com/terms-and-conditions-of-access.pdf>

This article may be used for research, teaching and private study purposes. Any substantial or systematic reproduction, re-distribution, re-selling, loan or sub-licensing, systematic supply or distribution in any form to anyone is expressly forbidden.

The publisher does not give any warranty express or implied or make any representation that the contents will be complete or accurate or up to date. The accuracy of any instructions, formulae and drug doses should be independently verified with primary sources. The publisher shall not be liable for any loss, actions, claims, proceedings, demand or costs or damages whatsoever or howsoever caused arising directly or indirectly in connection with or arising out of the use of this material.

## Electronic transport properties of liquid gallium–germanium alloys

M. MAYOUFI<sup>†</sup>, F. SAR<sup>‡</sup>, L. ANNO<sup>‡</sup> and J. G. GASSER<sup>\*‡</sup>

<sup>†</sup>Laboratoire de Chimie des Matériaux Inorganiques,

Université Badji-Mokhtar Annaba, BP12, 23000 Annaba, Algérie

<sup>‡</sup>Laboratoire de Physique des Milieux Denses (L.P.M.D), Université Paul Verlaine-Metz,  
1 boulevard ARAGO, CP 87811 57078 METZ cedex 3, France

(Received 31 August 2006; in final form 2 July 2007)

Germanium is a semiconductor in the solid state, but is a metal when it is molten. In the present work, the electrical resistivity and the absolute thermoelectric power (Seebeck coefficient) of the liquid  $\text{Ga}_{1-x}\text{Ge}_x$  alloys have been measured at 11 different concentrations as functions of temperature. Two different quartz cells fitted with tungsten and tungsten–rhenium electrodes have been used. Our experimental design is described. Experimental results have been compared with the calculations based on the Faber–Ziman formalism.

*Keywords:* Resistivity; Thermoelectric power; Liquid; Alloy; Gallium–germanium

### 1. Introduction

The purpose of this article is to measure the electrical resistivity and absolute thermoelectric power of liquid  $\text{Ga}_x\text{Ge}_{1-x}$  alloys in the whole concentration range. Germanium is a semiconductor in the solid state. But, when it is molten, it has metallic character. It is interesting to alloy of this element with gallium, which has a metallic behaviour in the both solid and liquid state and has a very low melting point (29.8°C). Thus it will be possible to study liquid Ga–Ge alloys at the temperature lower than the of melting point germanium. Makradi *et al.* [1] and Ben Hassine *et al.* [2] have investigated the resistivity and the thermoelectric power of pure germanium and gallium, respectively. To the authors' knowledge, no measurement has been made for Ga–Ge before this study. We recall in section 2 the definition of resistivity and thermoelectric power. In section 3 we describe briefly the experimental method that was used. Finally, in section 4, we present our experimental results and compare them to a theoretical calculation.

---

\*Corresponding author. Tel.: +33(0)387315859. Fax: 33(0)387315884. Email: gasser@univ-metz.fr

## 2. Theory

### 2.1. The electronic transport coefficients

If the electrical and thermal conductivity are in general well understood, it is not the case of the thermoelectric effects (Peltier, Thomson and Seebeck) that are more complex since a thermal effect is linked to an electrical cause and reciprocally. The electronic transport coefficients and the equations between them are well described in the book “Electronic Conduction in Solids” of Smith, *et al.* [3]. The specific case of the thermopower of metals and metallic alloys is described in Barnard’s [4] book “Thermoelectricity in Metals and Alloys”. The terminology used below is that used by these authors.

In a conductor, a potential gradient  $\overrightarrow{\nabla V}$  creates a density of current  $\vec{J}$ . At zero temperature gradient, it defines  $\sigma(\vec{J} = -\sigma\overrightarrow{\nabla V})$ . A temperature gradient  $\overrightarrow{\nabla T}$  creates a density of heat flux  $\vec{Q}$ . At zero density of current it defines  $\lambda(\vec{Q} = -\lambda\overrightarrow{\nabla T})$ . Crossed effects exist: a temperature gradient creates an electric field (Seebeck effect). The Seebeck coefficient is noted as  $S$  and is defined by:  $-\overrightarrow{\nabla V} = S\overrightarrow{\nabla T_K}$ . A density of current creates a density of heat flux (Peltier effect). The Peltier coefficient is  $\pi$ .

The three thermoelectric effects (Peltier, Seebeck and Thomson) are linked by the two Kelvin’s laws:

$$\pi = T_K S \quad \text{and} \quad h = T_K \frac{dS}{dT_K}. \quad (1 \text{ and } 2)$$

The thermal conductivity is linked to the electrical conductivity and to the Seebeck coefficient. A simplified expression is called the Wiedemann–Franz law. More details are given in [5].

### 2.2. Absolute thermoelectric coefficients measured in the laboratory

An experimental problem arises from the fact that one cannot measure the Seebeck coefficient (or thermopower or thermoelectric power or absolute thermoelectric power) and the Peltier coefficient of an element (pure metal or alloy). One can only measure the difference of two “absolute thermoelectric powers” of two elements by realising a “(thermo)-couple”. It is also the case for the Peltier effect. To get the “absolute” thermopower of an element, it is necessary to measure the electromotive force of a couple having that element by deriving it with respect to temperature and then by subtracting the known “absolute” thermopower of the second element, constituting the couple. Thus, it is necessary to know the absolute thermoelectric power of at least one element. This has been made possible thanks to the second Kelvin’s law. Indeed the Thomson coefficient is the only “absolute” coefficient of an element which is directly measurable (it does not need a junction). If a current passes through a wire where a temperature gradient exists, a release or absorption of heat appears, proportional to the Thomson coefficient. The experimental determination is, however, very difficult since the Thomson heat (for metals), proportional to the current  $I$ , is in general about 100 times lower than the quadratic Joule effect. The Thomson effect is measured by very accurate calorimetry, changing the direction of the current  $I$ . The Seebeck coefficient (absolute thermopower) is obtained from the second Kelvin’s law by

integrating the Thomson coefficient from 0 K to the considered temperature. Roberts *et al.* [6], at the National Bureau of Standards, measured the Thomson coefficient of very pure platinum (called “platinum 67”) from 0 K to 1600°C in a work which needed many years and many calorimeters (calorimetric measurements near 0 K need evidently a different calorimeter than that at 1900 K). Thanks to this work, we have the absolute thermopower of pure “platinum 67”. All the other elements are calibrated by realising a couple with platinum 67. At our laboratory we calibrate systematically all wires that we use for thermoelectric measurements. In this work we calibrate pure tungsten and tungsten-26% rhenium.

### 2.3. Calculation

The resistivity ( $\rho$ ) and the thermoelectric power ( $S$ ) have been calculated, using the Faber–Ziman formalism [7], under the following assumptions:

- (1) The structure of the alloys is approximated by the hard-sphere solution of the Percus–Yevick equation [8,9];
- (2) The electron–ion interaction is described by the volume-dependent model potential of Ashcroft [10]. The resistivity of a pure metal is given by the formula

$$\rho = \frac{3\pi^2 m^2 \Omega_0}{e^2 h^3 k_F^2} \int_0^1 a(\mathbf{q}) v^2(\mathbf{q}) 4 \left( \frac{\mathbf{q}}{2k_F} \right)^3 d \left( \frac{\mathbf{q}}{2k_F} \right) \quad (3)$$

where  $\Omega_0$  is the mean atomic volume and  $\mathbf{q}$  is the scattering wave vector.

For liquid alloys, the term  $a(\mathbf{q}) v^2(\mathbf{q})$  is replaced by [4]:

$$c_1 v_1^2 [1 - c_1 + c_1 a_{11}(\mathbf{q})] + c_2 v_2^2 [1 - c_2 + c_2 a_{22}(\mathbf{q})] + 2c_1 c_2 v_1 v_2 [a_{12}(\mathbf{q}) - 1]. \quad (4)$$

The  $a_{ij}$  ( $i, j = 1$  or  $2$  for a binary alloy) are the set of “Faber–Ziman” [7] hard-sphere partial structure factors [7,11] and the model potentials in the alloy are given by [8]  $v_i(\mathbf{q}) = (-2E_F/3)(\lambda^2 \cos(2k_F R_i x)/x^2 \varepsilon(\mathbf{q}))(Z_i/Z)$  where  $x = \mathbf{q}/2k_F$ ,  $\lambda^2 = \pi(a_0 k_F)^{-1}$ ,  $a_0$  is the Bohr radius,  $E_F$  is the Fermi energy,  $Z$  is the mean valence  $Z_i$  the valence of element  $i$  and  $\varepsilon(\mathbf{q})$  is the dielectric screening function. The core parameters  $R_i$  ( $i = 1, 2$  for two constituents) entering in the model potential have been fitted on the experimental values of the resistivity of pure metals, with Vashishta–Singwi [12] screening function.

The Seebeck coefficient may be written in the form:

$$S = \frac{\pi^2 k_B^2 T_k}{3|e|E_F} \chi \quad \text{with} \quad \chi = E_F \left( \frac{\partial \ln \rho(E)}{\partial E} \right)_{E_F} \quad (5 \text{ and } 6)$$

where  $k_B$  is the Boltzmann constant and is the dimensionless so-called “thermoelectric parameter”. Gasser [13,14] adapted the formalism to liquid alloys where we add an index  $i$  to characterise each constituent of the alloy. As for the resistivity with core radius  $R_i$ , the thermoelectric parameter  $\chi$ , hence the thermopower  $Q$ , is written in term of  $\Gamma_i$  [14,15] which are fitted on experimental values. The parameters  $\Gamma_i$  take into account the energy dependence of the Ashcroft model potential parameter  $R_i$ .

### 3. Experimental method

The experimental results presented in this article were obtained with two different devices, which measure jointly the electrical resistivity and the absolute thermopower. They combine a measurement of the electrical resistivity using a four-point probes technique and a measurement of the absolute thermoelectric power, employing a small  $\Delta T$  method [5]. The liquid metal is contained in fused silica cell (figures 1 and 2) provided with sealed tungsten/tungsten-26w% rhenium electrodes. The wires are used after calibrating their absolute thermopower with platinum 67 *versus* temperature and

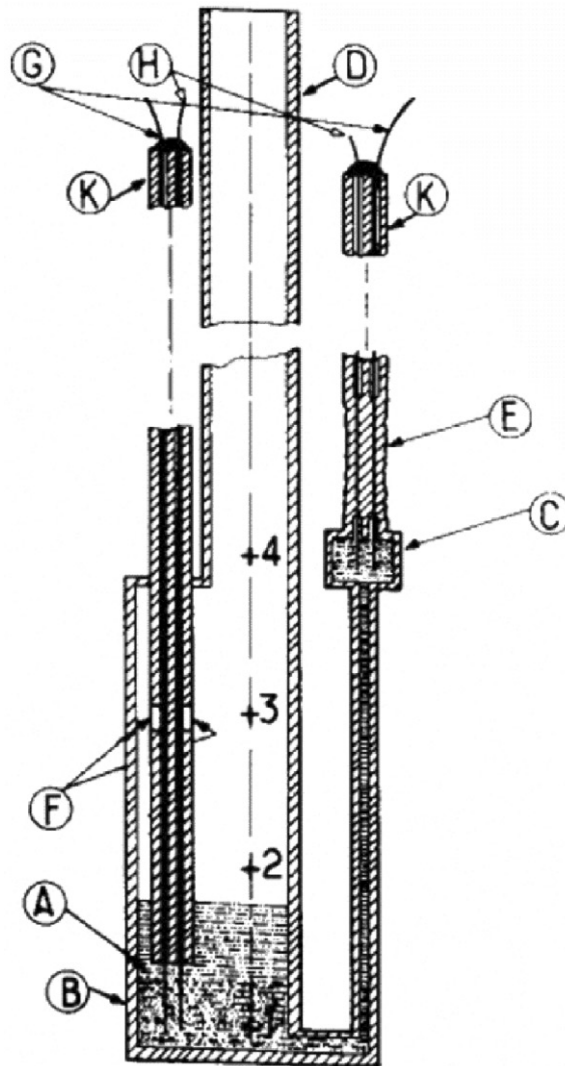


Figure 1. Classical cell. A: Molten metal; B: Main tank; C: Auxiliary tank; D: Tube for vacuum or pressure; E: Quartz-tungsten sealing; F: Holes to avoid the capillarity; G: Current electrodes; H: Voltage electrodes; K: Bifilarly tubes; 1, 2, 3, 4: Position of the thermocouples.

their e.m.f. *versus* temperature with a standard platinum/platinum-rhodium<sub>10w%</sub> thermocouple for temperature measurement. The tungsten/tungsten-26w% rhenium electrodes are sealed in the quartz. An auxiliary heater is placed in order to generate a temperature gradient between the two tanks. In order to put the liquid metal in the capillary, one has to first melt the metal grains under vacuum. When the metal is in liquid static, a small argon pressure applied in the main tube is sufficient to push the liquid in to the small tank. When a bubble appears, one applies vacuum in the main tube. This generates a movement of the liquid and eliminates the bubble. Another method to eliminate bubbles is to increase the argon pressure over the sample; the bubbles are reduced until they have a negligible size thus a negligible effect on the resistivity. The problem of this cell is that distillation arises when a metal is molten under vacuum and has a high vapour pressure. This is not the case for gallium and germanium. We developed a new kind of cell (symmetrical cell: figure 2) and compared the resistivity of the two cells. Two main tanks are linked by a capillary. Metal grains are molten under argon pressure. Then, the pressure on one side was increased and pushed the liquid into the other tank. We used this alloy to test this new kind of cell

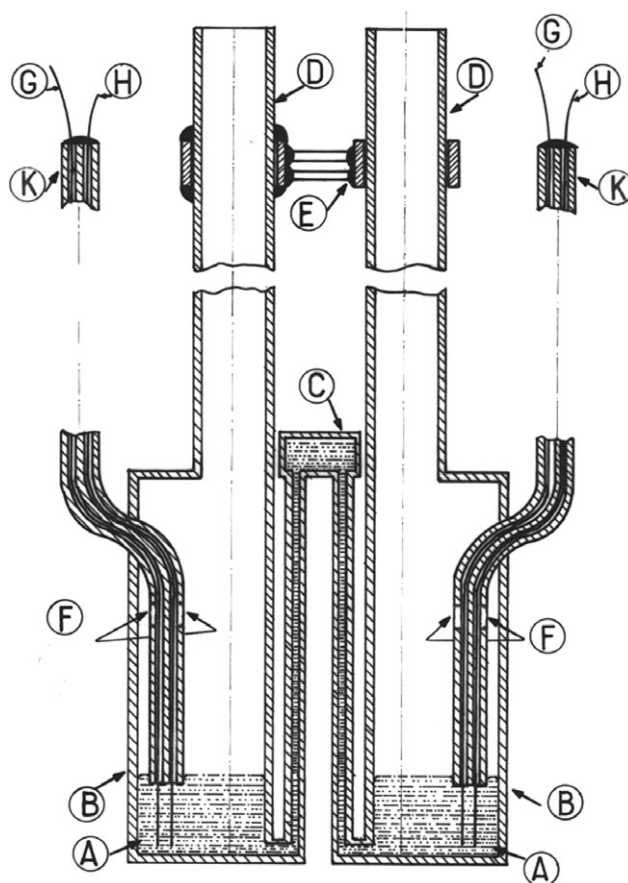


Figure 2. Symmetric cell. A: Molten metal; B: Main tanks; C: Auxiliary tank; D: Tubes for vacuum or pressure; E: support; F: Holes to avoid the capillarity; G: Current electrodes; H: Voltage electrodes; K: Bifilarly tubes.

suitable for high vapour pressure metals and obtained very similar results. This new cell also allows us to remove bubbles and to push metal into the capillary by moving the liquid from one tank to the other by applying a small differential pressure on each. In the first cell it is necessary to apply vacuum to remove the liquid from the capillary or to mix the alloy. But by doing this we can distillate the high vapour pressure alloys and modify the composition. In the second cell the liquid is pushed from one tank to the other by applying a small differential pressure, but remains under a high common static pressure. With this cell it is never necessary to apply vacuum, this technique avoids distillation. The two kinds of cell have been used in this work. All the results were comparable.

With all these cells to measure a resistivity, we measure, in fact, a resistance whose value is  $R = \int_0^L \rho (dl/S(l))$ . For a cylindrical wire we have  $R = \rho(L/S)$ . Since the capillary has not a regular shape, the geometrical constant of the cell is defined by  $C = \int_0^L \rho (dl/S(l))$ ,  $L$  is the length of the capillary and  $S(l)$  is the section of the conductor (which is not constant). An accurate determination of  $C$  by measuring the dimension of the cell is not possible. Thus the constant  $C$  was calibrated by measuring the resistance of the cell filled with triple-distilled mercury whose resistivity is well known. The relative uncertainty  $\Delta(\rho)/\rho$  in the final results is estimated to be no more than  $\pm 0.5\%$  for the resistivity. For the thermoelectric power, the total uncertainty is smaller than  $\pm 0.6 \mu\text{V K}^{-1}$ . The most important part comes from the calibration of the Seebeck coefficient of our wires and from Roberts *et al.* [6] determination of the thermopower of the reference (pure platinum). In both cases the uncertainty is estimated to  $\pm 0.2 \mu\text{V K}^{-1}$ . Another cause of uncertainty is that due to the electrical measurements ( $\pm 0.2 \mu\text{V K}^{-1}$ ). The metals that we employed were purchased from Johnson Matthey<sup>®</sup> Company with purity of 99.999% for gallium (Cu < 1 ppm, Mg < 1 ppm, Si < 1 ppm) and with a purity of 99.999% for germanium (Cu < 1 ppm, In < 1 ppm). The experimental details are given in [16].

## 4. Experimental results

### 4.1. Resistivity

Measurements have been carried out at 11 different compositions. Figure 3 shows the results of the resistivity *versus* temperature. The resistivity of gallium increases with temperature and the resistivity of germanium too. The behaviour is not far from a linear function of temperature for all the compositions. Our resistivity values have been fitted by a second order polynomial whose parameters are presented in table 1. The resistivity of  $\text{Ga}_{100-x}\text{Ge}_x$  *versus* concentration of gallium has been plotted at seven different temperatures (from 500 to 1100°C) in figure 4. We present in figure 5 the different results of numerical calculations at 950°C and compared them to our experimental curve. We first calculate the resistivity as a function of the parameter  $R_i$  of the Ashcroft empty core potential. Two values of  $R_i$  exactly give the experimental resistivity for each pure metal. The question is to make a choice of the good parameter. We obtained  $R_i = 0.5478$  and  $0.6345 \text{ \AA}$  for gallium at 950°C and  $R_i = 0.4831$  and  $0.6431 \text{ \AA}$  for germanium at the same temperature. The four possible calculated curves are plotted in figure 5. Two of them are convex and represent pretty well the resistivity of the alloy and the two others are concave. We will now compare the thermoelectric results.

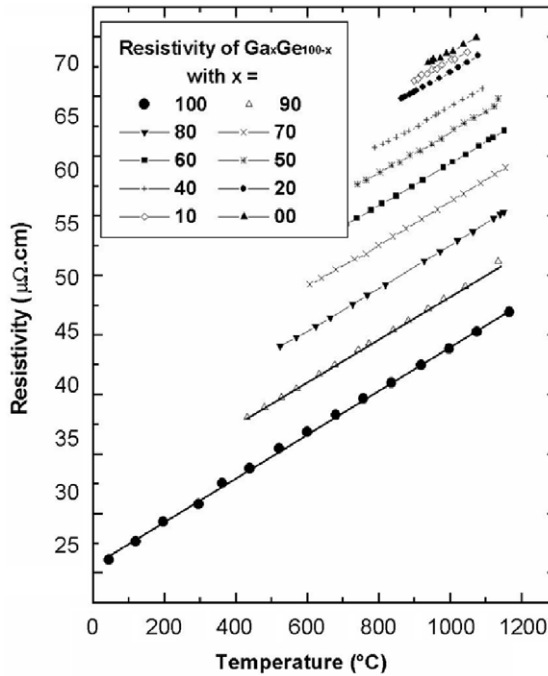


Figure 3. Experimental resistivity of  $\text{Ga}_x\text{Ge}_{100-x}$  as function of temperature at different germanium concentrations  $x$ .

Table 1. Coefficients of the polynomial fit to the electrical resistivities of liquid  $\text{Ga}_{100-x}\text{Ge}_x$  alloys:  
 $\rho = A_0 + A_1 T_C + A_2 T_C^2$  ( $\mu\Omega \text{ cm}$ ).

Composition	$A_0$	$A_1 \times 10^3$	$A_2 \times 10^6$	Temperature range ( $^{\circ}\text{C}$ )	Correlation coefficient
Ga	25.2558	19.91	-1.25406	45–1167	0.9997
$\text{Ga}_{90}\text{Ge}_{10}$	30.7741	16.40	1.23905	431–1135	0.9996
$\text{Ga}_{80}\text{Ge}_{20}$	35.2406	16.07	1.18979	524–1150	0.9999
$\text{Ga}_{70}\text{Ge}_{30}$	39.8558	14.04	2.23326	607–1155	0.9998
$\text{Ga}_{60}\text{Ge}_{40}$	43.7721	13.13	2.50101	676–1152	0.9999
$\text{Ga}_{50}\text{Ge}_{50}$	185.8670	-34.10	41.93570	805–1090	0.9999
$\text{Ga}_{40}\text{Ge}_{60}$	50.8119	09.34	3.95639	789–1090	0.9990
$\text{Ga}_{20}\text{Ge}_{80}$	57.9827	00.82	8.22718	864–1078	0.9999
$\text{Ga}_{10}\text{Ge}_{90}$	45.6270	29.09	-6.72898	450–800	0.9925
Ge	74.55147	-27.21	21.36440	938–1073	0.99351

#### 4.2. Thermoelectric power

Figure 6 shows the absolute thermoelectric power of liquid  $\text{Ga}_x\text{Ge}_{100-x}$  as a function of temperature. The thermopower is negative and decreasing with temperature in the whole temperature range for all compositions. The thermopower has been fitted by a first order polynomial whose parameters are represented in table 2. The thermoelectric power of pure gallium is not very different from that of pure germanium. Two concentration ranges can be distinguished. In the first one, from pure gallium to  $\text{Ga}_{70}\text{Ge}_{30}$ , the thermopower remains nearly constant when the concentration of germanium increases. In the germanium-rich side of the phase diagram the



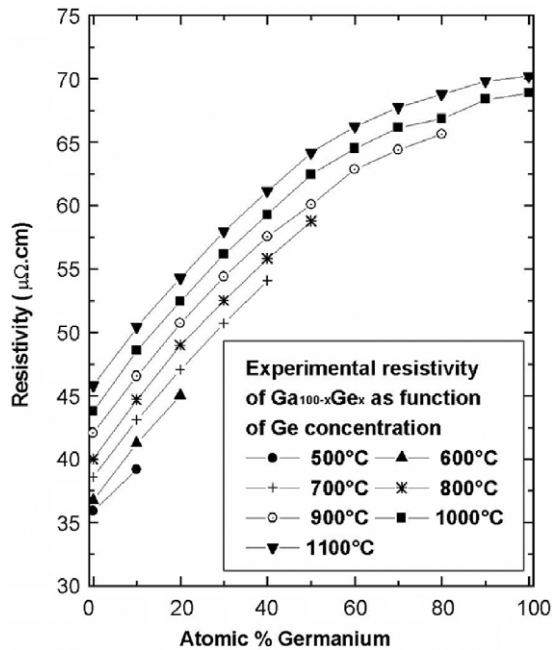


Figure 4. Experimental resistivity of  $\text{Ga}_{100-x}\text{Ge}_x$  at 500, 600, 700, 800, 900, 1000 and 1100°C as function of concentration.

thermopower decreases with the gallium concentration. A discontinuity appears at 40%, but taking into account the accuracy of the experiment, it is difficult to conclude to an anomalous physical phenomenon. We plotted in figure 7 the thermoelectric power of the alloy at 950°C *versus* concentration of germanium. We compare them with calculated values. As in [14] we determined for each value of  $R_i$  a value of a second parameter  $\Gamma_i$  in order to fit exactly the thermopower of pure germanium and gallium with the couple of parameters  $R$  and  $\Gamma$ . We obtain again four curves that exactly fit the experimental thermopower of the pure metals but the concentration curves can be very different. It appears clearly that the  $R_i$  determinations which gave the best results for the resistivity also give the best results for the thermopower when alloying. Reasonable results are obtained with  $R_i=0.6413 \text{ \AA}$  for germanium, both for resistivity and for thermopower.  $R_i=0.5478 \text{ \AA}$  for gallium gives a slightly better result for the thermopower, while  $R_i=0.6345 \text{ \AA}$  gives a slightly better result for the resistivity. The two curves are convex for the resistivity, like the experimental resistivity and concave for the thermopower, like the experimental thermopower. The accuracy of the calculation at equiatomic concentration is better than 10% for the resistivity and  $0.5 \mu\text{V K}^{-1}$  for the thermopower, which is excellent.

## 5. Conclusion

Two different quartz cells have been used in the resistivity and thermoelectric power measurements. They allowed us to study the Ga–Ge alloys in the whole composition

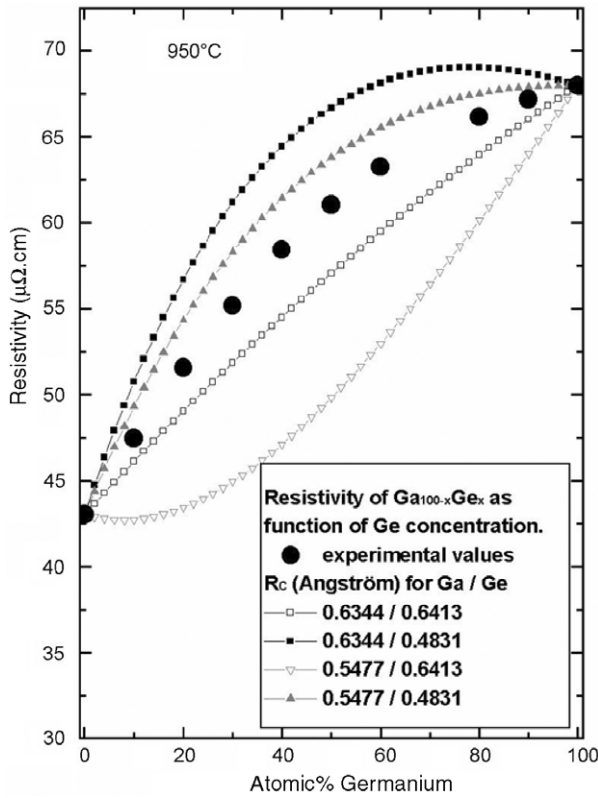


Figure 5. Resistivity of  $\text{Ga}_{100-x}\text{Ge}_x$  as function of germanium concentration at  $950^\circ\text{C}$ . Comparison of the experimental curve to the calculated ones using different values of Ashcroft parameters  $R_i$  fitting the resistivity of pure metals.

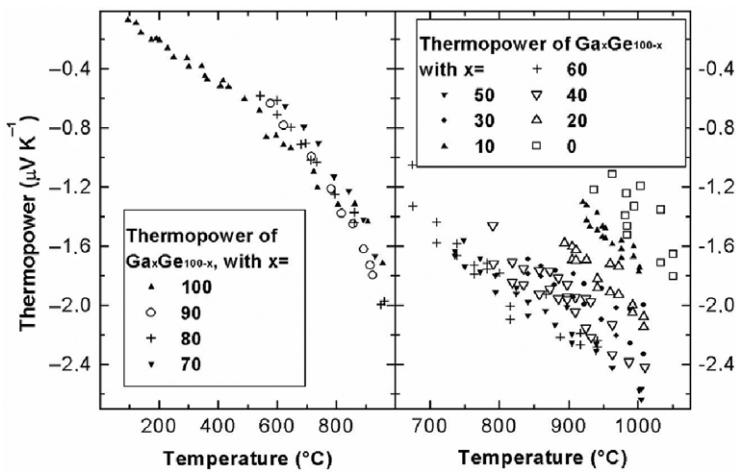


Figure 6. Experimental Seebeck coefficient of  $\text{Ga}_x\text{Ge}_{100-x}$  as function of temperature at different germanium concentrations  $x$ .

Table 2. Coefficients of the polynomial fit to the Seebeck coefficient of liquid  $\text{Ga}_{100-x}\text{Ge}_x$  alloys:  
 $S = A_0 + A_1 T_C + A_2 T_C^2$  ( $\text{VK}^{-1}$ ).

composition	$A_0$	$A_1 \times 10^3$	$A_2 \times 10^6$	Temperature range ( $^{\circ}\text{C}$ )	Correlation coefficient
Ga	0.39503	-2.09	0	550–956	-0.97949
Ge	0.01262	-0.96578	-0.793045	550–956	0.99122
$\text{Ga}_{90}\text{Ge}_{10}$	1.28157	-3.25	0	550–924	-0.99321
$\text{Ga}_{80}\text{Ge}_{20}$	1.38165	-3.38	0	550–960	-0.98002
$\text{Ga}_{70}\text{Ge}_{30}$	1.43287	-3.23	0	550–930	-0.98695
$\text{Ga}_{60}\text{Ge}_{40}$	0.3253	-2.1	0	550–941	0.95497
$\text{Ga}_{50}\text{Ge}_{50}$	0.91413	-3.43	0	550–1004	-0.97011
$\text{Ga}_{40}\text{Ge}_{60}$	1.30039	-3.65	0	550–1010	-0.91912
$\text{Ga}_{30}\text{Ge}_{70}$	0.63901	-2.8	0	550–1070	-0.84679
$\text{Ga}_{20}\text{Ge}_{80}$	2.22166	-4.26	0	550–1008	-0.91333
$\text{Ga}_{10}\text{Ge}_{90}$	2.89551	-4.62	0	550–1000	0.92389
Ge	3.49686	-4.89	0	550–1050	-0.70466

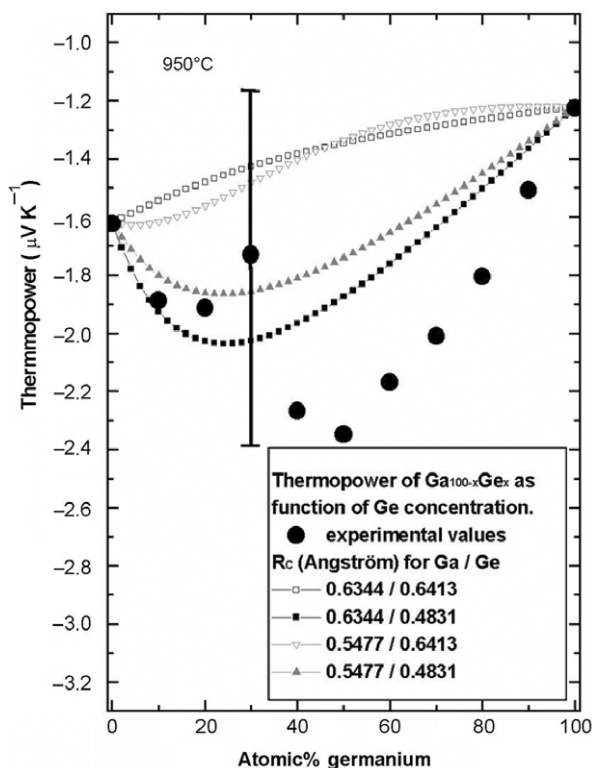


Figure 7. Thermopower of  $\text{Ga}_{100-x}\text{Ge}_x$  as function of germanium concentration at  $950^{\circ}\text{C}$ . Comparison of the experimental curve to the calculated ones using different values of  $R_i$  and  $\Gamma_i$  fitting the thermopower of pure metals.

range and in a large temperature range. The concept of our cell permits us to control and prevent bubbles from appearing in the liquid alloys by applying an argon pressure or a difference of pressure between the two tanks. A new cell, allowing high vapour pressure alloy to be measured, has been tested satisfactorily and has been compared to

classical cell. Measurements are quite accurate for both resistivity (about 0.5%) and thermoelectric power ( $\pm 0.6 \mu\text{V K}^{-1}$ ). The resistivity values are very regular. Numerical calculations give pretty good results for this alloy.

On the basis of a phenomenological model fitted on the electronic transport properties of pure metals, the alloying behaviour is represented within 3–4% for resistivity and  $\pm 0.4 \mu\text{V K}^{-1}$  for the thermopower.

## References

- [1] A. Makradi, J.G. Gasser, J. Hugel, A. Yazı, M. Bestandji. *J. Phys. Condens. Matter*, **11**, 671 (1999).
- [2] L.B. Hassine, J. Auchet, J.G. Gasser. *Phil. Mag. B*, **82**, 1225 (2002).
- [3] A.C. Smith, J.F. Janak, R.B. Adler. *Electronic Conduction in Solids*, McGraw-Hill Series in Phys. Quant. Electronics (1967).
- [4] R.D. Barnard. *Thermoelectricity in Metals and Alloys*, p. 30, Taylor and Francis, London (1972).
- [5] F. Sar, J.G. Gasser. *Intermetallics*, **11**, 1369 (2003).
- [6] R.B. Roberts, F. Righini, R.C. Compton. *Phil. Mag. B*, **52**, 1147 (1985).
- [7] T.E. Faber. *An Introduction to the Theory of Liquid Metals*, Cambridge University Press, Cambridge (1972).
- [8] J.K. Percus, G.J. Yevick. *Phys. Rev.*, **110**, 1 (1958).
- [9] N.W. Ashcroft, J. Lekner. *Phys. Rev.*, **145**, 83 (1966).
- [10] N.W. Ashcroft. *Phys. Lett.*, **23**, 48 (1966).
- [11] N.W. Ashcroft, D.C. Langreth. *Phys. Rev.*, **159**, 500 (1967).
- [12] P. Vashishta, K.S. Singwi. *Phys. Rev. B* **6**, 875 (1972).
- [13] J.G. Gasser. Thèse d'Etat. Université de Metz (1982).
- [14] A. Bath, J.G. Gasser, J.L. Bretonnet, R. Bianchin, R. Kleim. *J. Phys. C*, **8**, 519 (1980).
- [15] N.W. Ashcroft. *J. Phys. C (Proc. Phys. Soc.)*, **1**, 232 (1968).
- [16] L. Anno. Mémoire d'ingénieur, CNAM, Metz (1985).